

Two-dimensional electron gas and persistent photoconductivity in $\text{Al}_x\text{Ga}_{1-x}\text{N}/\text{GaN}$ heterostructures

T. Y. Lin, H. M. Chen, M. S. Tsai, and Y. F. Chen

Department of Physics, National Taiwan University, Taipei, Taiwan, Republic of China

F. F. Fang

Center for Condensed Matter Sciences, National Taiwan University, Taipei, Taiwan, Republic of China

C. F. Lin and G. C. Chi

Department of Physics, National Central University, Chung-Li, Taiwan, Republic of China

(Received 23 September 1997; revised manuscript received 18 May 1998)

We present results of electrical and optical measurements in an $\text{Al}_x\text{Ga}_{1-x}\text{N}/\text{GaN}$ heterostructure. The presence of a two-dimensional electron gas at the high-quality $\text{Al}_x\text{Ga}_{1-x}\text{N}/\text{GaN}$ heterointerface is confirmed by Shubnikov–de Haas measurement, which shows well-resolved magnetoresistance oscillations starting in fields below 3 T at 1.3 K. From the temperature dependence of the oscillation amplitude, the obtained effective mass $(0.24 \pm 0.02)m_0$ is in excellent agreement with the value of cyclotron resonance measurements in two-dimensional (2D) systems, but larger than the values of theoretical and experimental results in GaN bulk films. We point out that the effective-mass enhancement in 2D systems is due to the effects of band nonparabolicity and wave-function penetration into the barrier material. The results of photoconductivity measurements reveal that persistent photoconductivity (PPC) does exist in the $\text{Al}_x\text{Ga}_{1-x}\text{N}/\text{GaN}$ heterostructure, and that the PPC behavior of $\text{Al}_x\text{Ga}_{1-x}\text{N}/\text{GaN}$ heterojunction is quite different from that of the GaN epitaxial thin films. A possible mechanism is presented to interpret the observed PPC effect. [S0163-1829(98)07843-7]

I. INTRODUCTION

GaN-based wide-band-gap III-V nitride semiconductors currently attract extensive attention for their device applications, such as UV-blue-light-emitting diodes, short-wavelength laser diodes, and high-temperature field effect transistors.^{1–5} High-quality $\text{Al}_x\text{Ga}_{1-x}\text{N}/\text{GaN}$ heterostructures have been shown to contain two-dimensional electron gas (2DEG),^{6–8} and are investigated for high-temperature device application. Although assessment of the properties of $\text{Al}_x\text{Ga}_{1-x}\text{N}/\text{GaN}$ heterostructures is actively pursued to accelerate the device fabrication, detailed studies on several important parameters such as the electrical and optical properties associated with defects have not been explored. Further advances in the performance of GaN-based heterostructure devices are expected to occur with an improved understanding in material properties. In this paper, we present the results of electrical and photoconductive studies of an $\text{Al}_x\text{Ga}_{1-x}\text{N}/\text{GaN}$ heterostructure with the buffer layer containing an excess GaN/ $\text{Al}_x\text{Ga}_{1-x}\text{N}$ superlattice. Shubnikov–de Haas (SdH) oscillations have been employed to ensure that a 2DEG exists in the studied sample. Well-resolved magnetoresistance oscillations can be observed down to a relatively low value of the magnetic field (3 T), indicating the heterointerface to be of rather good quality. From the temperature dependence of the oscillation amplitude, the determined effective mass has a value of $(0.24 \pm 0.02)m_0$, where m_0 is the mass of a free electron. This value is in excellent agreement with the recent reports obtained from cyclotron-resonance measurements^{8,9} in GaN/ $\text{Al}_x\text{Ga}_{1-x}\text{N}$ heterostructures, but larger than the theoretical and experimental values in GaN bulk films. We attribute this discrepancy to the effects of nonparabolicity and hybridization of well and barrier band parameters. In the

study of photoconductivity, we found that the persistent photoconductivity (PPC) effect does exist in $\text{Al}_x\text{Ga}_{1-x}\text{N}/\text{GaN}$ heterostructure, and that it strongly depends on the temperature. The PCC effect disappears at room temperature, which is quite different from that of the GaN epitaxial films.^{10,11} This behavior implies that different mechanisms are responsible for the PPC effects in $\text{Al}_x\text{Ga}_{1-x}\text{N}/\text{GaN}$ heterostructures and bulk GaN thin films. Through studies under various conditions, a possible mechanism is proposed to interpret the observed PPC effect in an $\text{Al}_x\text{Ga}_{1-x}\text{N}/\text{GaN}$ heterostructure.

II. SAMPLE PREPARATION

A high-quality $\text{Al}_x\text{Ga}_{1-x}\text{N}/\text{GaN}$ heterostructure was grown by metal-organic chemical-vapor deposition on (0001) 6H-SiC substrates. We choose the (0001) silicon face, for which each Si atom has a single dangling bond at the surface. The (0001)_{Si} SiC were degreased in sequential ultrasonic baths of acetone for 30 min and rinsed in deionized water, then cleaned by the cleaning procedure developed by Radio Corporation of America (RCA).¹² Heavy metals were removed using a heated (80 °C) $\text{H}_2\text{SO}_4:\text{HNO}_3$ solution. Next, a surface oxide was grown in a 60 °C $\text{HCl}:\text{H}_2\text{O}_2:\text{H}_2\text{O}$ (5:3:2) solution to passivate the Si dangling bonds, in a manner analogous to that for Si substrates.¹³ This grown oxide was then stripped with a diluted (10:1) $\text{H}_2\text{O}:\text{HF}$ solution. After a final HF dip, the SiC substrates were blown dry with N_2 prior to the regrowth. During the growth the SiC substrate was placed on a graphite susceptor in a horizontal-type reactor with a rf heater. Triethylgallium (TEGa), Trimethylaluminum (TMA), and ammonia (NH_3) were used as the Ga, Al, and N sources, respectively. The mole flow rate of TEG and TMA sources is 3.37 and 0.78 $\mu\text{mol}/\text{min}$ for

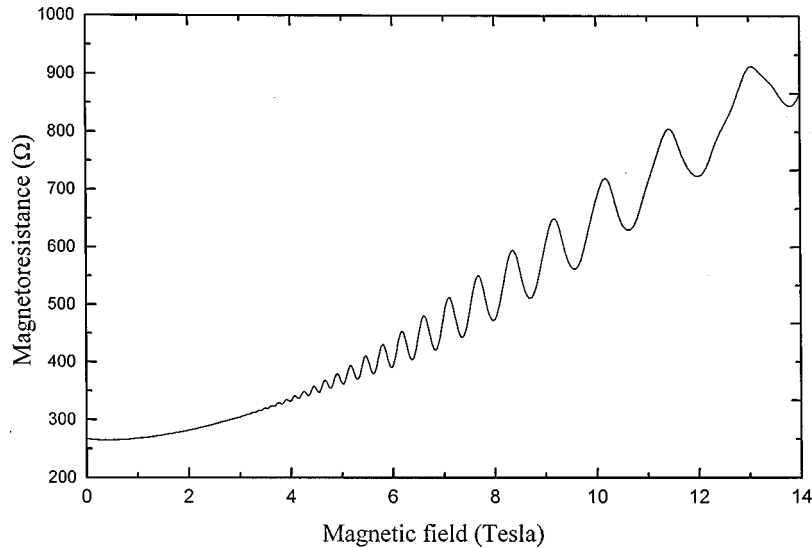


FIG. 1. The Shubnikov–de Haas oscillations of magnetoresistivity from 0 to 15 T at 1.3 K.

grown $\text{Al}_{0.08}\text{Ga}_{0.92}\text{N}$ epitaxial layers. The carrier gas is hydrogen (H_2), and the growth pressure was kept at 76 torr. Before growing GaN films, the SiC substrates were treated by thermal baking at 1100°C , to clean the contamination on the SiC. Then the temperature was decreased to 1025°C to grow five pairs of GaN/ $\text{Al}_{0.08}\text{Ga}_{0.92}\text{N}$ with a layer thickness of $100\text{ \AA}/100\text{ \AA}$. These buffer layers were used for strain relief prior to the growth of a $1.3\text{-}\mu\text{m}$ GaN epitaxial layer. An $\text{Al}_x\text{Ga}_{1-x}\text{N}$ layer (500 \AA) was then grown on top of the GaN, and finally a $100\text{-}\text{\AA}$ GaN cap layer to prevent the oxidation of the $\text{Al}_x\text{Ga}_{1-x}\text{N}$ layer. The full width at half maximum of the x ray is 145 arc s for the thick layer of GaN ($1.3\text{ }\mu\text{m}$). This value is smaller than we previously reported for a GaN epitaxial layer grown on a sapphire substrate.¹⁴ The sheet carrier density and the electron mobility were measured using the van der Pauw technique of the usual low-field Hall measurement apparatus. Ohmic contacts were formed by depositing the indium drop to the four corners of the samples, and annealing the sample at 400°C for 10 s. The obtained carrier density and mobility at 77 K are $5.48 \times 10^{12}\text{ cm}^{-2}$ and $4708\text{ cm}^2/\text{V s}$, respectively. These values are typical for all high-quality $\text{Al}_x\text{Ga}_{1-x}\text{N}/\text{GaN}$ heterostructures available to data.^{6–8} The carrier concentration remains constant in the temperature range between 77 and 1.3 K. It is a clear signature that the electrons are derived from modulation doping. The Hall mobility is relatively constant. It increases slightly up to $5500\text{ cm}^2/\text{V s}$ at 1.3 K. It indicates that the low temperature scattering is not dominated by the local impurities, more evidence of barrier-mediated electron transfer in this 2DEG system.¹⁵

III. RESULTS AND DISCUSSION

A. Shubnikov–de Haas measurement

For the SdH measurements, a He^4 cryostat inserted in a superconducting magnet was used. The sample was carefully and slowly cooled in the dark. Low noise ac phase-sensitive detection techniques were employed. Care was taken that the probing signal was sufficiently small to ensure that no hot-electron effect was present down to the lowest temperature.

A typical high-magnet field (0–15 T) magnetoresistance at 1.3 K is shown in Fig. 1. Well-resolved magnetoresistance oscillations starting in fields as low as 3 T can be clearly observed. The appearance of SdH patterns occurs at a lower magnetic field than those in previous reports.^{6–8} The SdH oscillatory resistivity has been used to identify the existence of a 2DEG in the GaN heterojunction.⁷ However, the 2D character of the conducting carriers needs to be further confirmed by performing magnetoresistance measurements at different angles (θ) of the magnetic field inclined with respect to the sample growth direction. For a 2D system, the relationship between the oscillatory period and the direction of the magnetic field should obey the $\cos\theta$ rule. Our measurement indeed follows this rule nicely.¹⁶ Thus our result firmly establishes that a 2DEG exists in the GaN/ $\text{Al}_x\text{Ga}_{1-x}\text{N}$ heterostructure. Because no intentional doping was incorporated during the crystal growth, the 2DEG could be located at both sides of the $1.3\text{-}\mu\text{m}$ GaN interfaces. From the fact that the barrier layers on both sides are different, i.e., one is bulk $\text{Al}_x\text{Ga}_{1-x}\text{N}$ and the other is an $\text{Al}_x\text{Ga}_{1-x}\text{N}/\text{GaN}$ superlattice, we expect that these two heterojunctions should have quite different properties. If there are 2DEG's on both interfaces, they should have different carrier densities. However, our SdH spectrum only contains one period, indicating that the 2DEG is located at one of the interfaces. In order to identify the exact location of the 2DEG, we have fabricated three $\text{Al}_x\text{Ga}_{1-x}\text{N}/\text{GaN}$ heterostructures with different $\text{Al}_x\text{Ga}_{1-x}\text{N}$ layers. These three different $\text{Al}_x\text{Ga}_{1-x}\text{N}$ structures (each with a thickness of 500 \AA) are the $\text{Al}_{0.08}\text{Ga}_{0.92}\text{N}$ bulk structure; the compositional stair-step structure, and the graded composition structure above $1.3\text{-}\mu\text{m}$ undoped GaN epitaxial layers. It is found that the 2DEG properties can be changed by different $\text{Al}_x\text{Ga}_{1-x}\text{N}$ structures.¹⁷ Because the interface with the superlattice layer is far away from the $\text{Al}_x\text{Ga}_{1-x}\text{N}$ layer, it is hardly influenced by the change of the $\text{Al}_x\text{Ga}_{1-x}\text{N}$ structure. We therefore conclude that the 2DEG is located at the $\text{Al}_x\text{Ga}_{1-x}\text{N}$ (500 \AA) and GaN interfaces.

The SdH oscillation allows us to determine accurately the 2D carrier concentration by measuring the periods of the oscillation in $1/B$ which is in turn equal to $e/(hn_s)$, where e ,

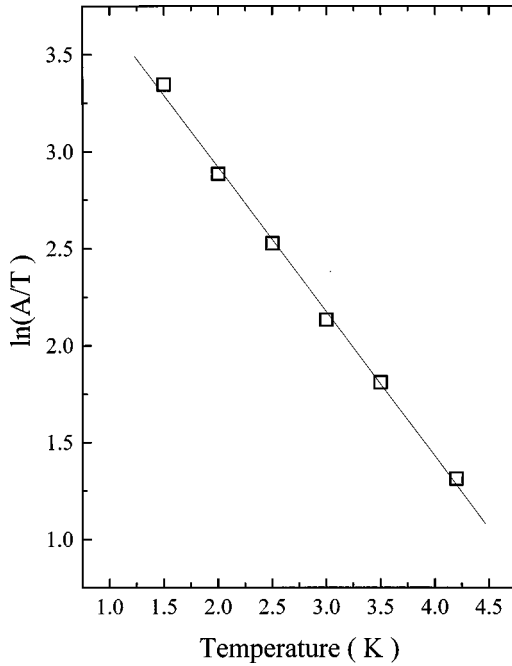


FIG. 2. The plot of $\ln(A/T)$ against T at the field of 5 T. The line is the best fit to the data.

h , and n_s are electronic charge, Planck constant, and the areal carrier concentration, respectively. The obtained carrier concentration is $4.55 \times 10^{12} \text{ cm}^{-2}$ at 1.3 K, which is slightly less than that obtained from the Hall-effect measurement, indicating the existence of parallel conduction. The effective mass of the 2DEG can be determined by the temperature dependence of the oscillating amplitude by the equation,¹⁸

$$\frac{A(T)}{A(T_0)} = \frac{T_0 \sinh(2\pi^2 kT/\hbar\omega_c)}{T \sinh(2\pi^2 kT_0/\hbar\omega_c)}, \quad (1)$$

where $\hbar\omega_c = \hbar eB/m^*$, and m^* is the effective mass. If we approximate $\sinh(2\pi^2 kT/\hbar\omega_c)$ by $\exp(2\pi^2 kT/\hbar\omega_c)$, the oscillating amplitude can be written as

$$\ln\left(\frac{A}{T}\right) \approx c - \frac{2\pi^2 km^*}{e\hbar B} T, \quad (2)$$

where c does not depend on temperature. Thus, if we plot $\ln(A/T)$ versus T at a fixed magnetic field, the effective mass m^* can be obtained from the slope of the straight line; the result is plotted in Fig. 2. The effective mass has been evaluated at several values of the magnetic field, and the results give an average value of $m^* = (0.24 \pm 0.02)m_0$. This is in excellent agreement with the value obtained by the cyclotron-resonance measurement of 2DEG confined at a GaN/Al_xGa_{1-x}N interface.^{8,9} This result further confirms the fact that the 2DEG is on the GaN side of the heterojunction.

Even though the above measured effective mass is consistent with cyclotron-resonance measurements, it is higher than the recent theoretical results, which calculated values slightly below $0.2m_0$.^{19,20} Because the studied GaN/Al_xGa_{1-x}N heterostructure has a relatively high carrier concentration, it is possible that nonparabolicity effects may contribute to the enhancement of the effective mass, as suggested by Knap *et al.*⁸ Theoretically, the effective-mass en-

hancement in a triangular well can be approximately estimated by Ando's formulation²¹

$$\frac{\Delta m^*}{m_b^*} = [(1 + 4(\langle K \rangle + E_F)/E_g)]^{1/2} - 1, \quad (3)$$

where $\langle K \rangle$ and E_F denote the kinetic energy and the Fermi energy in the ground subband, respectively, and $\langle K \rangle$ is given approximately as $E_1/3$. E_1 is the energy of the ground subband, E_g is the band gap, and m_b^* is the band-edge effective mass. The Fermi energy can be determined by

$$E_F = \frac{\pi \hbar^2 n}{m^*}, \quad (4)$$

where the electron concentration n and the effective mass m^* can be obtained from the above measurements. The obtained Fermi energy is 46 meV.

The energy of the first subband can be estimated from a self-consistent calculation of the energy-band potential and energy levels at the heterointerfaces, as reported by Bergman *et al.*²² In the calculation we used $m^* = 0.24m_e$, a GaN energy gap of 3.5 eV, an Al_xGa_{1-x}N energy gap of 3.8 eV, and a conduction-band-offset coefficient $Q_c = 0.80$.²³ The calculated energy of E_1 is 153 meV above the bottom of the potential notch. Substituting the values of $E_F = 46$ meV and $E_1 = 153$ meV into Eq. (3); the obtained band-edge effective mass $m_b^* = (0.22 \pm 0.02)m_0$. This value is still slightly higher than the theoretical result,^{19,20} and this discrepancy has been attributed to the polaron correction.²⁴ However, it has been pointed out that the effective mass may not be affected by the polaron interaction, due to the strong screening effect of the 2DEG.^{9,25} Since the band offset (~ 300 meV) in our studied sample is rather small, we believe that the wave function in the triangular well can easily penetrate into the barrier layer. We therefore suggest that the origin of the remaining discrepancy can be attributed to the hybridization of the well and barrier band parameters, which has been adopted to explain the effective-mass enhancement in other III-V heterostructures.^{26,27} It has been shown, in narrow quantum wells or at a small confinement energy, that the nonparabolicity always underestimates the enhanced effective mass, and the increase in effective mass is mainly connected to barrier leakage of the electron wave function.

B. Photoconductivity measurement

For photoconductivity (PC) measurements, a tungsten lamp dispersed by a monochromator was used as the photoexcitation light source. For the PPC, a He-Cd or an Ar-ion laser was used as the photoexcitation light source. The sample was attached to a copper sample holder and placed inside a closed-cycle He refrigerator with care, to ensure good thermal contact yet electrical isolation. The data obtained under different conditions were taken in such a way that the system was always allowed to relax to equilibrium. This was to ensure that the data obtained had the same initial condition. A bias of 20 eV was supplied and the conductivity was measured by a Keithley 236 source measure unit. Detailed of the PC measurement procedure were similar to those described previously.^{28,29}

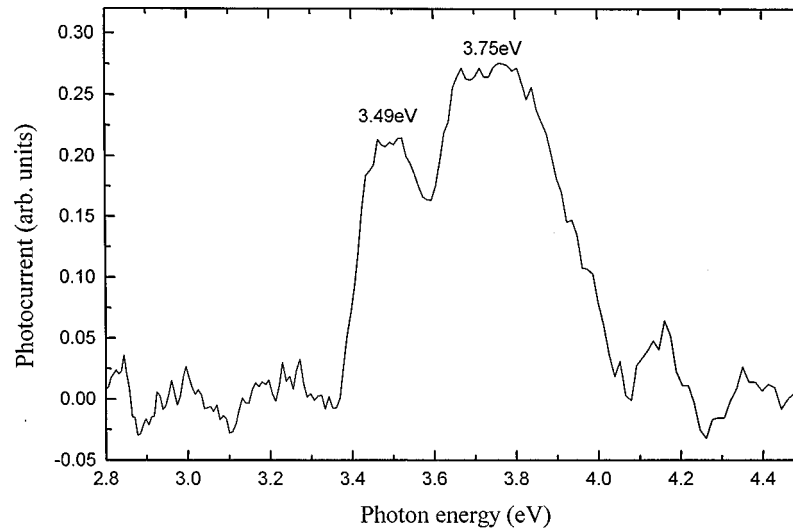


FIG. 3. Photoconductivity spectrum of the $\text{Al}_x\text{Ga}_{1-x}\text{N}/\text{GaN}$ heterostructure taken at 12 K.

Figure 3 shows the resulting PC spectrum of the $\text{Al}_x\text{Ga}_{1-x}\text{N}/\text{GaN}$ heterostructure at 12 K. The PC effect of the $\text{Al}_x\text{Ga}_{1-x}\text{N}/\text{GaN}$ heterostructure is slightly different from that of the bulk GaN.²⁷ In the case of bulk GaN, only one sharp peak near the GaN band edge at 3.49 eV is observed, while in the case of an $\text{Al}_x\text{Ga}_{1-x}\text{N}/\text{GaN}$ heterostructure, one additional peak near the $\text{Al}_x\text{Ga}_{1-x}\text{N}$ band edge at 3.75 eV is also observed. This is consistent with our photoluminescence measurement.¹⁶ A rather interesting feature of the photoresponse in the $\text{Al}_x\text{Ga}_{1-x}\text{N}/\text{GaN}$ heterostructure is the observation of the PPC effect as shown in Fig. 4. From Fig. 4 we can see that the conductivity increased gradually after the sample is exposed to light. After the light is removed, there is a sudden decrease in light-induced conductivity, and then the rest of the light-induced conductivity persists for a very long period of time, which can extend to more than 10^6 s. The phenomenon of the PPC effect has been observed in many III-V and II-VI semiconductor thin films and heterostructures.²⁸⁻³³ The investigation of the PPC

effect has led to an understanding of the carrier relaxation and metastability of crystal defects, which are very important for academic interest and technological application. Recently, the PPC effect has also been observed in *p* and *n*-type GN thin films.^{10,11,33} Here we report that the PPC effect can also occur in an $\text{Al}_x\text{Ga}_{1-x}\text{N}/\text{GaN}$ heterostructure.

In order to explore the properties of the PPC effect in an $\text{Al}_x\text{Ga}_{1-x}\text{N}/\text{GaN}$ heterostructure further, we performed a measurement of the temperature dependence. It is found that the PPC effect strongly depends on the temperature, and it disappears for the temperature above 150 K. This behavior is quite different from that of bulk GaN thin films.^{10,11,33} For GaN thin films, the PPC effect can be clearly observed at room temperature. The long-term relaxation in Fig. 4 does not follow an exponential function; instead it can be described by the stretched exponential relation

$$I_{\text{PPC}}(t) = I_{\text{PPC}}(0) \exp[-(t/\tau)^\beta], \quad (5)$$

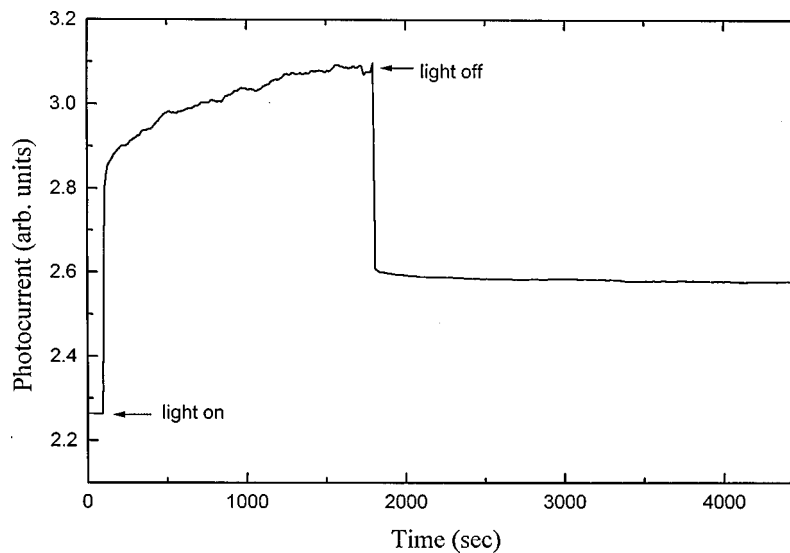


FIG. 4. A typical buildup and decay behavior of persistent photoconductivity in an $\text{Al}_x\text{Ga}_{1-x}\text{N}/\text{GaN}$ heterostructure at 12 K. The spectrum was excited by a He-Cd laser, working at 325 nm.

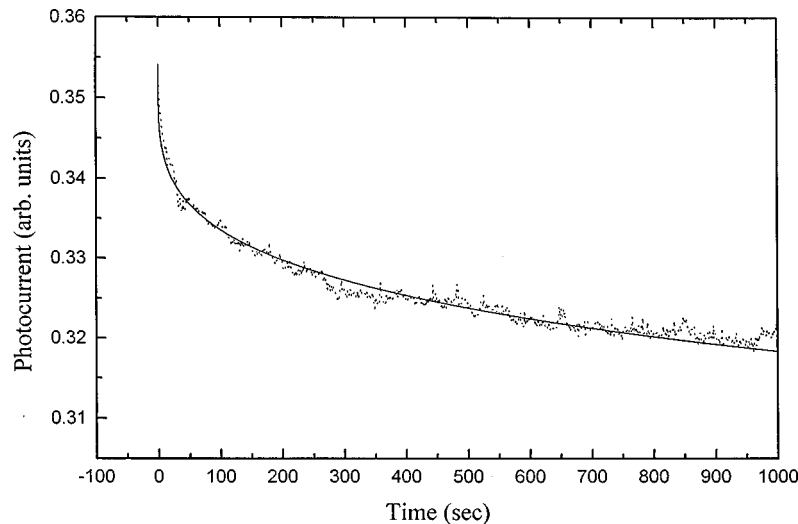


FIG. 5. Comparison of PPC decay kinetics with a stretched-exponential function. The solid dots are the measured data at 12 K, and the solid curve is the least square fit of Eq. (5).

where $I_{\text{PPC}}(0)$ is the PPC buildup level near the moment of light excitation being removed, τ is the PPC decay time constant, and β is the decay exponent. Figure 5 displays the comparison between the experimental data and Eq. (5), in which the fitted values of β and τ are 0.25 and 7.28×10^6 s, respectively. The temperature dependence of τ can be described by

$$\tau = \tau_0 \exp[\Delta E/kT], \quad (6)$$

where ΔE is the carrier capture barrier. The obtained value of ΔV is 2.7 meV, which is quite different from that of the bulk value 132 meV.^{29,33} Because the PPC effects in an $\text{Al}_x\text{Ga}_{1-x}\text{N}/\text{GaN}$ heterostructure and GaN thin films have very different properties, it implies that the underlying mechanisms responsible for the PPC effects are also different. To confirm this result further, we replaced the HeCd laser by an Ar-ion laser as the excitation source, which can pass through the $\text{Al}_x\text{Ga}_{1-x}\text{N}$ layer and excite defect levels in GaN layer. We found that similar to the PPC effect in bulk GaN films,^{10,11,31} the PPC effect now can be observed at room temperature. In GaN thin films, the PPC effect has been attributed to the metastable behavior of intrinsic defects.⁷ Here we propose that the PPC effect in an $\text{Al}_x\text{Ga}_{1-x}\text{N}/\text{GaN}$ heterostructure can be understood as follows. When electron-hole pairs are created in the $\text{Al}_x\text{Ga}_{1-x}\text{N}$ layer due to photoexcitation, electrons travel across the $\text{Al}_x\text{Ga}_{1-x}\text{N}/\text{GaN}$ interface and fall into the triangular well in the GaN side, and they contribute to the PC response. The remaining holes are trapped by shallow defects near the $\text{Al}_x\text{Ga}_{1-x}\text{N}/\text{GaN}$ interface, which leads to the spatial separation of photoexcited electrons and holes, and thus the PPC effect occurs. This proposed model can explain all of the

above observed PPC behaviors quite well. Given the fact that a significant advancement of our understanding in $\text{Al}_x\text{Ga}_{1-x}\text{As}$ heterostructures through the studies of PPC effect, we expect that additional investigation following the results shown here should be able to enhance our understanding of the electrical and optical properties in $\text{Al}_x\text{Ga}_{1-x}\text{N}/\text{GaN}$ heterostructures.

IV. CONCLUSION

In conclusion, we employed Shubnikov-de Haas measurement to confirm that a two-dimensional gas (2DEG) can be observed in high quality $\text{Al}_x\text{Ga}_{1-x}\text{N}/\text{GaN}$ heterointerface. The effective mass $(0.24 \pm 0.02)m_0$ of 2DEG obtained from the temperature dependence of the oscillating amplitude is in excellent agreement with the values determined by cyclotron-resonance measurements in $\text{GaN}/\text{Al}_x\text{Ga}_{1-x}\text{N}$ heterostructures, but larger than the theoretical and experimental values in GaN bulk films. We suggest that the effective-mass enhancement of a 2DEG is due to the effects of nonparabolicity and wave-function penetration into the barrier layer. The results of photoconductivity measurements reveal that persistent photoconductivity does exist in the $\text{Al}_x\text{Ga}_{1-x}\text{N}/\text{GaN}$ heterostructure, and that the PPC behavior strongly depends on the temperature. We found that the PPC behavior of the $\text{Al}_x\text{Ga}_{1-x}\text{N}/\text{GaN}$ heterojunction is quite different from that of the GaN epitaxial thin films. A possible mechanism responsible for the observed PPC effect is also proposed.

ACKNOWLEDGMENT

This work was partially supported by the National Science Council of the Republic of China.

¹I. Akasaki, H. Amano, M. Kito, and K. Hiramatsu, *J. Lumin.* **48**, 666 (1991).

²S. Nakamura, T. Mukai, and M. Senoh, *Appl. Phys. Lett.* **64**, 1687 (1994).

³H. Morkoc, S. Strite, G. B. Gao, M. E. Lin, B. Sverdlov, and M.

Burns, *J. Appl. Phys.* **76**, 1363 (1994).

⁴S. Nakamura, S. Senoh, N. Iwasa, S. Nagahama, T. Yamada, T. Matsushita, H. Kiyoku, and Y. Sugimoto, *Jpn. J. Appl. Phys., Part 2* **35**, L74 (1996).

⁵Ozgur Aktas, Z. F. Fan, S. N. Mohammad, A. E. Botchkarev, and

- H. Morkoc, *Appl. Phys. Lett.* **69**, 3872 (1996).
- ⁶M. A. Khan, Q. Chen, C. J. Sun, M. S. Shur, and B. Gelmont, *Appl. Phys. Lett.* **67**, 1429 (1995).
- ⁷J. M. Redwing, M. A. Tischler, J. S. Flynn, S. Elhamri, M. Ahoujja, R. S. Newrock, and W. C. Mitchel, *Appl. Phys. Lett.* **69**, 963 (1996).
- ⁸W. Knap, S. Contreras, H. Alause, C. Skierbiszewski, J. Camassel, M. Dyakonov, J. L. Robert, J. Yang, Q. Chen, M. Asif Khan, M. L. Sadowski, S. Huant, F. H. Yang, M. Goiran, J. Leotin, and M. S. Shur, *Appl. Phys. Lett.* **70**, 2123 (1997).
- ⁹Y. J. Wang, R. Kaplan, H. K. Ng, K. Doverspike, D. K. Gaskill, T. Ikedo, I. Akasaki, and H. Amono, *J. Appl. Phys.* **79**, 8007 (1996).
- ¹⁰H. M. Chen, Y. F. Chen, M. C. Lee, and M. S. Feng, *Phys. Rev. B* **56**, 6942 (1997).
- ¹¹C. H. Qiu and J. I. Pankove, *Appl. Phys. Lett.* **70**, 1983 (1997).
- ¹²J. Sumakeris, Z. Sitar, K. S. Ailey-Trent, K. L. More, and R. F. Davis, *Thin Solid Films* **225**, 244 (1993).
- ¹³B. S. Meyerson, F. J. Himpsed, and K. J. Uram, *Appl. Phys. Lett.* **57**, 1034 (1990).
- ¹⁴C. F. Lin, G. C. Chi, M. S. Feng, J. D. Guo, J. S. Tsang, and H. H. Hong, *Appl. Phys. Lett.* **68**, 3758 (1996).
- ¹⁵H. L. Stormer, A. C. Gossard, W. Wiegmann, and K. Baldwin, *Appl. Phys. Lett.* **39**, 912 (1981).
- ¹⁶H. M. Chen, Master's thesis, National Taiwan University, 1997.
- ¹⁷C. F. Lin, H. C. Cheng, J. A. Huang, M. S. Feng, J. D. Guo, and G. C. Chi, *Appl. Phys. Lett.* **70**, 2583 (1996).
- ¹⁸A. E. Stephens, R. E. Miller, J. R. Sybert, and D. G. Seiler, *Phys. Rev. B* **18**, 4394 (1978).
- ¹⁹T. Yang, S. Nakajima, and S. Sakai, *Jpn. J. Appl. Phys., Part 1* **34**, 5912 (1995).
- ²⁰M. Suzuki, T. Uenoyama, and A. Yanase, *Phys. Rev. B* **52**, 8132 (1995).
- ²¹T. Ando, *J. Phys. Soc. Jpn.* **51**, 3893 (1982).
- ²²J. P. Bergman, T. Lundström, B. Monemar, H. Amano, and I. Akasaki, *Appl. Phys. Lett.* **69**, 3456 (1996).
- ²³J. Baur, K. Meier, M. Kunzer, U. Kaufmann, and J. Schneider, *Appl. Phys. Lett.* **65**, 2211 (1994).
- ²⁴W. Knap, H. Alause, J. M. Bluet, J. Camassel, J. Young, M. Asif Khan, Q. Chen, S. Huant, and M. Shur, *Solid State Commun.* **99**, 195 (1996).
- ²⁵M. J. Yang, P. J. Lin-Chung, B. V. Shanabrook, J. R. Waterman, R. J. Wagner, and W. J. Moore, *Phys. Rev. B* **47**, 1691 (1993).
- ²⁶C. Wetzel, Al. L. Efros, A. Moll, B. K. Meyer, P. Omling, and P. Sobkowicz, *Phys. Rev. B* **45**, 14 052 (1992).
- ²⁷Y. T. Dai, Y. F. Chen and I. Lo, *Phys. Rev. B* **55**, 5235 (1997).
- ²⁸L. H. Chu, Y. F. Chen, D. C. Chang, and C. Y. Chang, *J. Phys.: Condens. Matter* **7**, 4525 (1995).
- ²⁹H. M. Chen, Y. F. Chen, M. C. Lee, and M. S. Feng, *J. Appl. Phys.* **82**, 899 (1997).
- ³⁰D. V. Lang and R. A. Logan, *Phys. Rev. Lett.* **39**, 635 (1977).
- ³¹P. M. Mooney, *J. Appl. Phys.* **67**, R1 (1990).
- ³²H. X. Jiang and J. Y. Lin, *Phys. Rev. Lett.* **57**, 873 (1990).
- ³³J. Z. Li, J. Y. Lin, H. X. Jiang, A. Salvador, A. Votchkarev, and H. Morkoc, *Appl. Phys. Lett.* **69**, 1474 (1996).